Ceramics International 23 (1996) 361–366

PII: S0272-8842(96)00044-2
0272-8842/97 $17.00+0.00

The Si_3N_4 and Si_3N_4/TiC Layered Composites by Slip Casting

Chih-Hung Yeh & Min-Hsiung Hon

Department of Materials Science and Engineering (MAT32), National Cheng Kung University, Tainan, Taiwan

(Received 8 November 1995; accepted 31 January 1996)

Abstract: Layered composites in the Si_3N_4–TiC system, with monolithic Si_3N_4 as outer layers and Si_3N_4/TiC as inner core, were fabricated by slip casting and pressureless sintering. From zeta potential and viscosity measurements of Si_3N_4 and Si_3N_4/TiC suspensions, the conditions for the preparation of layered composites have been determined. During cooling from high temperature sintering, the difference in coefficients of thermal expansion between inner core and outer layer is expected to establish a compressive surface stress. Bar-shaped samples were indented using a Vickers indenter under loads ranging from 30 to 500 N on outer layers and were fractured in four-point bending. Layered composites of Si_3N_4–15 v/o TiC, with a thickness of 250 μm Si_3N_4 as outer layers, exhibit an excellent damage resistance, decreasing in strength only about 30% after indenting with a load of 500 N caused by the presence of a compressive surface stress of 325 MPa in the outer layer. © 1997 Published by Elsevier Science Limited

1 INTRODUCTION

Silicon nitride (Si_3N_4) is a promising engineering ceramic for high temperature structural application. Mechanical properties of monolithic Si_3N_4 can be enhanced by compositing with other materials. Owing to process problems and the cost of whiskers and fibres, however, increasing attention is being devoted to particulate composites. Recently, the TiC particulate (with high modulus, hardness and electrical conductivity), acting as a second phase dispersoid, has been incorporated into monolithic Si_3N_4 to improve not only the fracture toughness but also the electrical conductivity of composite ceramics.[1–6]

An attempt to establish compressive surface stresses for surface strengthening, ceramic layer-composites, such as SiC/AlN and Al_2O_3/ZrO_2,[7–13] has been developed using a material with high coefficient of thermal expansion (C.T.E) or large molar volume as outer layer in comparison to inner layer material. Upon cooling, the difference of C.T.E or molar volume between constrained inner and outer materials thereby creates a compressive surface stress on the outer layer. It was shown that the presence of compressive surface stress acts as a protective layer to exhibit an excellent damage and wear resistance providing an ideal basis for the ceramic cutting tool applications.[14] Numerous green-forming techniques including die pressing, slip casting, tape casting, as well as electrophoretic deposition, can be used to fabricate layered composites. Generally, the slip casting process is considered to be an advantageous shaping method for the production of components with complex geometry as well as uniform thickness.

Compressive surface stress of conventional three layer composites [Fig. 1(b)] formed by die pressing or tape casting are established only upon the two surface layers of the specimen. Thus, the function of protective surface layer for contact damage resistance exists only at the vertical directions of outer layers but parallel one. Compared with the method of die pressing and tape casting, slip casting caused by the advantage of fluidity of slips offer the feasibility for producing a novel layered composite whose outer layers can fully envelop the inner core [Fig. 1(a)]. The orientational problem of compressive surface stress of conventional three-layer (sandwich) composites can be eliminated by using slip casting instead of die pressing and tape casting to produce novel layered composites.

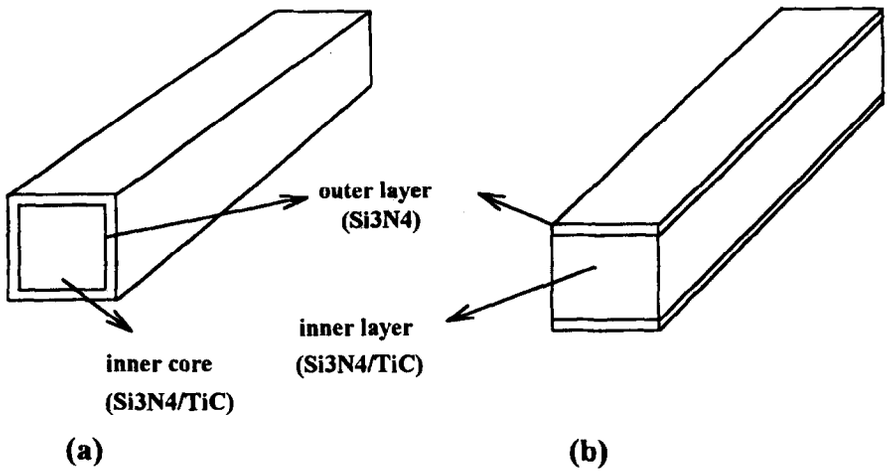

Fig. 1. Schematic diagram for the layered composites. (a) Conventional three-layer composite green compact formed by die pressing or tape casting. (b) Novel layered composite green compact formed by slip casting in this work, inner core enveloped by outer layer.

The objective of the present study is to investigate a powerful route: slip casting to produce Si_3N_4–TiC layered composites. As Si_3N_4 has a lower C.T.E ($\approx 3.2\times10^{-6}/°C$) and better oxidation resistance[6] compared to TiC (C.T.E$\approx 8\times10^{-6}/°C$), thus, by making monolithic Si_3N_4 as the outer layers and Si_3N_4/TiC as an inner core [Fig. 1(a)], a compressive surface stress can be established for improving damage resistance.

2 EXPERIMENTAL PROCEDURE

The starting powder mixtures of Si_3N_4 (SN-E10, particle size 0.3 μm, UBE, Tokyo, Japan), 5 wt% Y_2O_3 (grade fine C, particle size <1 μm, H. C. Stark, Goslar, FRG) and 2 wt% Al_2O_3 (AKP-20, particle size 0.5 μm, Sumitomo Co. Ltd, Japan) used in this study were mixed with various volume contents of TiC particulate (T-1227 and T-1150, for particle sizes 2 and 10 μm, respectively, CERAC, Wisconsin, USA). Colloidal stability of aqueous suspension was studied through zeta potential measurements (Zeta III, Zeta-Meter, USA) using 200 ppm concentration dispersion in 10^{-3} M KCl solution. To determine the zeta potential as a function of pH, the 10^{-2} N HCl and KOH solutions were used to adjust pH for desired values. An aqueous suspension of Si_3N_4/TiC powder mixtures with a solid content of 36 v/o using 0.2–0.5 wt% Darvan C (R. T. Vanderbuilt Co., Norwalk, CT) as defloccuant and pH 9.5–10.5 was prepared by ball milling. The corresponding viscosities were measured using a rotational viscometer (BL, Tokyo Keiki Co., Ltd, Japan) at 60 r.p.m.

The slips were then cast into plaster of Paris molds to make a solid cast bar. Wall thickness versus casting time was measured for drain casting. When the bodies were cast, they were carefully removed from the moulds and dried at room temperature for at least 24 h.

Cast specimens were pressureless sintered at 1775 °C for 4 h under 1 atm N_2 gas flow in a graphite furnace (FVPHP-R-5, Fujidempa, Japan). Density of the sintered specimens was measured using water immersion method. Specimens (5 cm×0.5 cm×0.5 cm) were tested for flexural strength using four-point bending method with inner and outer spans of 10 and 20 mm, respectively, and with a cross-head velocity 0.5 mm/min.

3 RESULTS AND DISCUSSION

3.1 Slip rheology and deflocculation

Figure 2 shows the zeta potential versus pH curves for both Si_3N_4 and TiC aqueous suspensions. The isoelectric points (IEP) of Si_3N_4 and TiC suspensions are at pH 7.2 and pH 2, respectively. According to the difference of IEP for the two phases, it is concluded that a difference in oxide surface structure is present. The low IEP of TiC suspension indicates that its surface contains more acidic sites compared to the high IEP of Si_3N_4 suspension based on the Lewis acid–base concept.[15] Colloidal stability is achieved at pH >10, where zeta potential values are high enough to obtain a deflocculated system.

Figure 3 shows the apparent viscosity of Si_3N_4–TiC slips with a solid loading of 36 v/o as a function of volume content and particle size of TiC. The apparent viscosity increases either with the increasing of volume content of TiC or the decreasing of particle size of TiC. Figure 4 shows the effect of volume content of TiC on the pH of

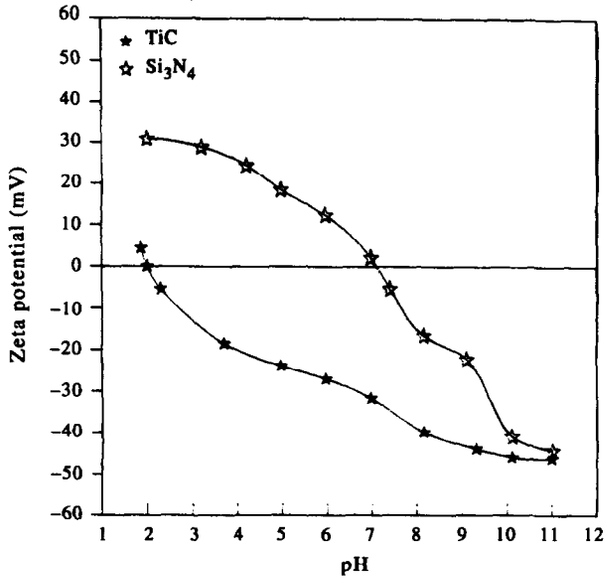

Fig. 2. Zeta potential vs pH for Si_3N_4 and TiC aqueous suspensions.

slips. Since Si_3N_4 milled or aged in water usually results in raising the pH caused by the dissociation of Si_3N_4 to form ammonia,[15] thus pH increases from 10 to 10.2 after ball milling for Si_3N_4 slip alone. The pH of slips decreases, however, with increasing the volume content of TiC, which could be because of the Lewis acid character on the surface of TiC. The pH decrease of the suspension by the addition of TiC dispersiod would result in the formation of flocculation and then increase the viscosity of slips (Fig. 3).

3.2 Sintering and mechanical properties

Compressive surface strength, σ_c, of three-layer composites is given by:[9–13]

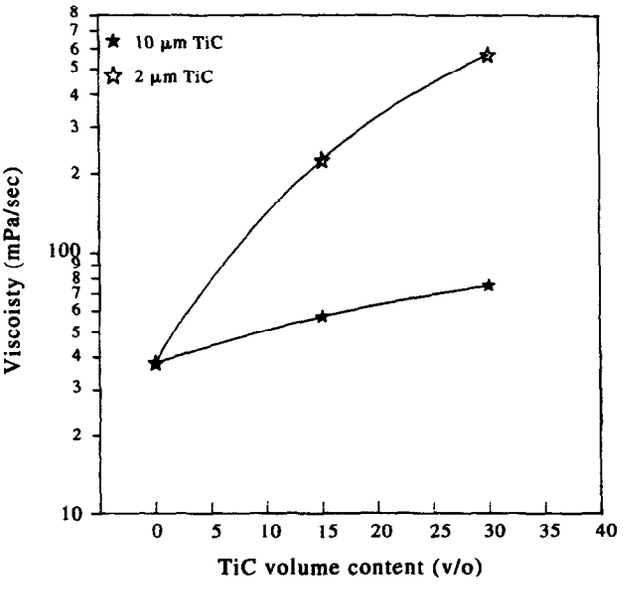

Fig. 3. The effect of volume content and particle size of TiC on the apparent viscosity of Si_3N_4–TiC slips.

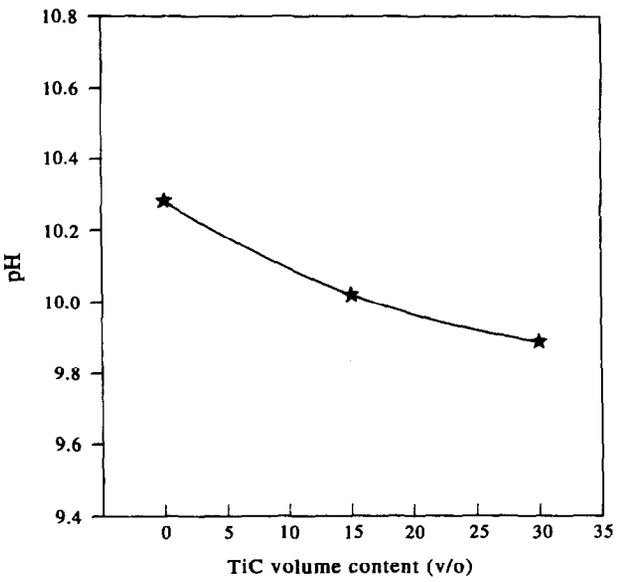

Fig. 4. The effect of volume content of TiC on the pH of slips after ball milling in Si_3N_4–TiC system. The initial pH value of slips is 10.

$$\sigma_c = \frac{-E_1 E_2 \Delta\varepsilon_o}{1-\nu)\left[2E_1\left(\frac{d_1}{d_2}\right)+E_2\right]} \quad (1)$$

where E_1 and E_2, d_1 and d_2 are the modulus and thickness of outer and inner layers, respectively. $\Delta\varepsilon_o$ is relative free strain between outer and inner layers, which depends on the difference of C.T.E of the inner and outer layers. For a fixed total thickness of the bar specimen, namely $2d_1 + d_2 =$ constant, and neglecting the small differences in elastic modulus, the compressive surface strength is mainly dependent on the difference of C.T.E, as well as the thickness of the outer layers. In general, a larger difference of C.T.E and thinner thickness of outer layers (i.e. lower d_1/d_2) causes a

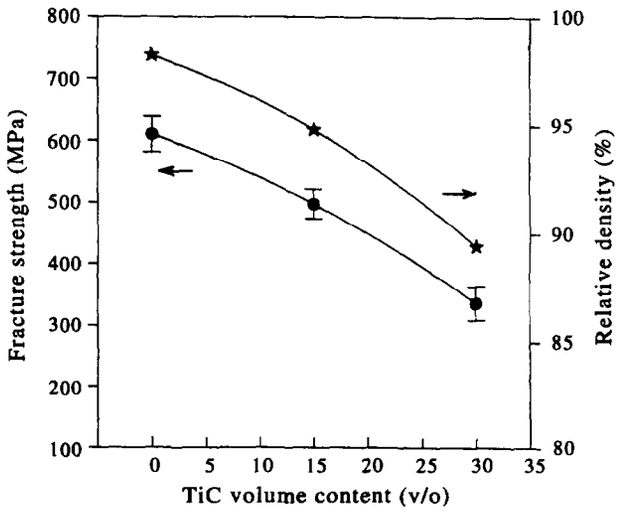

Fig. 5. The four-point bending strength and relative density as a function of the volume content of TiC in Si_3N_4–TiC specimens fabricated by slip casting and pressureless sintering.

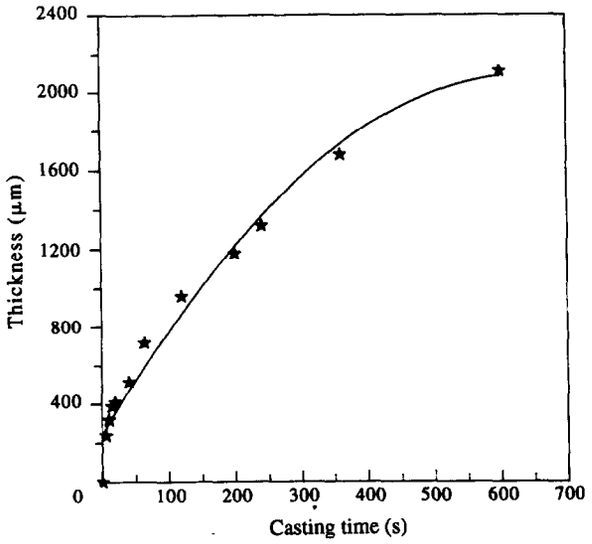

Fig. 6. Thickness vs casting time for green cast bodies of Si_3N_4.

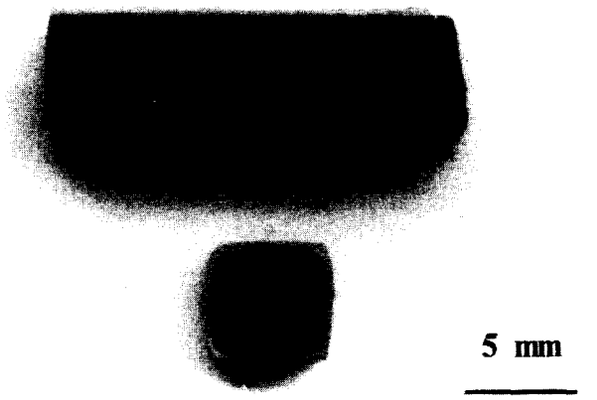

Fig. 7. Novel layered composites of Si_3N_4 (outer layer) and Si_3N_4–15 v/o TiC (inner core) produced by slip casting and pressureless sintering.

larger surface compressive stress. For the consideration of the oxidation resistance of the composite, the outer layers are composed of monolithic Si_3N_4. Therefore, the difference of C.T.E between inner core and outer layers is fully contributed by the amount of volume TiC content in the Si_3N_4/TiC inner core.

Since the Si_3N_4 doped with coarser TiC dispersoids yields a larger toughness[16] than that with fine dispersoids, thus 10 μm TiC is used in the inner core of Si_3N_4–TiC layered composites. Figure 5 is the relative density and four-point fracture strength as a function of volume content of 10 μm TiC. Compared with monolithic Si_3N_4, the fracture strength and relative density decrease with increasing volume content of TiC. The inner core, consisting of high volume content of TiC, is expected to generate a high compressive surface stress in the outer layers due to a larger difference of C.T.E between inner core and outer layers. The addition of 30 v/o of TiC, however, results in a fracture strength lower than 400 MPa, which is disadvantageous for using as an inner core material in layered composites. Thus, in this work Si_3N_4–15 v/o TiC is adopted as an inner core material.

The layer thickness of Si_3N_4 cake as a function of casting time is shown in Fig. 6. The desired thickness of the outer layers can be controlled by manipulating the casting rate of Si_3N_4 slip and considering the shrinkage fraction in pressureless sintering. For example, the outer layers thicknesses of 250 and 1000 μm were obtained by slips cast for 10 and 200 s and sintered at 17750 °C for 4 h, respectively. Figure 7 is a photograph of layered composites fabricated by slip casting and pressureless sintering. The inner core and outer layers of bar-shaped specimens with darker and lighter contrast are Si_3N_4–15 v/o TiC and monolithic Si_3N_4, respectively. As can be seen, the inner materials are enveloped by the outer layers.

Table 1 shows the strength of indented samples in the monolithic materials and the layered composites as a function of indent load. In contrast with the layered composite specimens, the single component of specimens abruptly decreases in strength with increasing indent load. The strengths of monolithic Si_3N_4 and Si_3N_4–15 v/o TiC composite ceramics decrease by about 72% and 73%, respectively, after indenting with a load of 500 N. Damage resistance of layered composites is related to the thickness of the outer layers, and as can be seen, the strength of layered composites is inactive to the indent load as the thickness of outer layers is

Table 1. Summarized data of indentation load dependence of fracture strength for the novel layered composites, inner core and outer layer materials in Si_3N_4–TiC system

Composition (v/o)		d_1 μm	Flexural strength (MPa)					
			Indent load (N)					
Outer layer (d_1)	Inner core (d_2)		0	30	50	100	300	500
Si_3N_4	Si_3N_4	0	613±54	442±36	417±25	262±22	188±26	170±17
Si_3N_4–15TiC	Si_3N_4–15Tic	0	498±48	314±27	291±29	243±26	159±19	134±24
Si_3N_4	Si_3N_4–15Tic	250	604±94	574±33	563±21	483±33	453±26	422±22
Si_3N_4	Si_3N_4–15Tic	1000	658±88	578±37	525±30	423±21	365±16	322±12

Total thickness ($d=2d_1+d_2$) of the bar specimen is 5 mm.

decreasing. For example, the layered composite of Si_3N_4–15 v/o TiC with a thickness of 250 μm Si_3N_4 as outer layers exhibits an excellent damage resistance, decreasing in strength only about 30% after indentation with a load of 500 N. Figure 8 shows the fractographs of a fractured monolithic Si_3N_4 and a layered composite. In the monolithic Si_3N_4, the fracture surface is uniform over the entire cross-section. On the contrary, the fracture surface of the layered composite is relatively smooth in the outer layer region but, however, is rough in the inner core region. The sudden change in fracture topography between outer layer and inner core suggests that the state of stresses abruptly changes from surface compression stress into central tensile stress.

The dependence of indent load, P, on the fracture strength, σ, of the indented samples is described as below:[17]

$$\sigma = AP^{-B} \tag{2}$$

$$\log\sigma = \log A - B\log P \tag{3}$$

where A is a constant for a sample with a half-penny-shaped crack,[13] B is related to the capability of crack growth resistance of a material. Generally, B is approximately 1/3 for ceramics,[12,13,18,19] such as Al_2O_3, Si_3N_4 and SiC, etc.

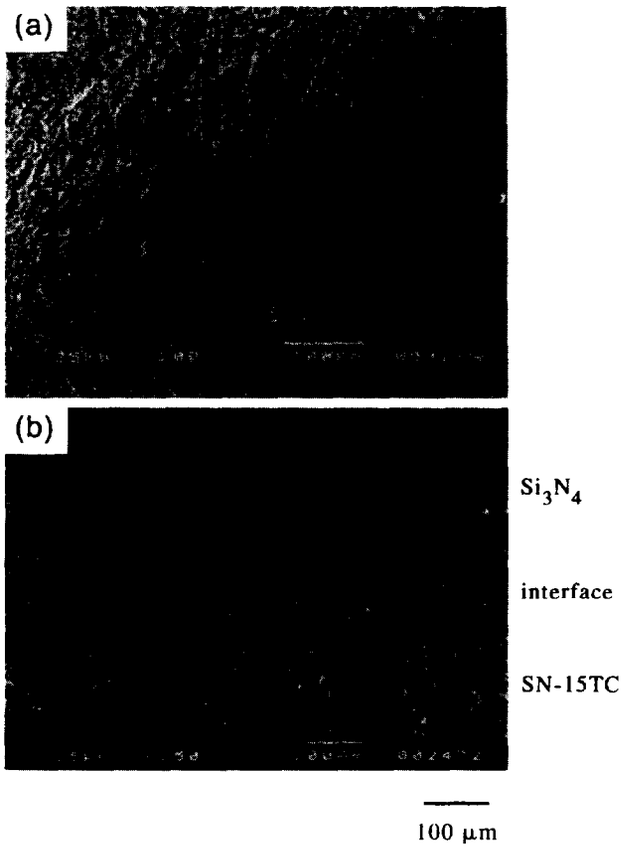

Fig. 8. Fractographs of (a) fractured monolithic Si_3N_4 and (b) layered composite.

Figure 9 shows logarithmic plots of four-point bending strength of indented bars vs indent load for monolithic Si_3N_4 and Si_3N_4–15 v/o TiC ceramics. Slopes of both lines are close to $-1/3$ (namely B equal to 1/3). Based on the evidences of damage tolerance in Si_3N_4–TiC layered samples (Table 1), the enhanced fracture stress for Si_3N_4–TiC layered samples compared with monolithic Si_3N_4 (outer layer material) and Si_3N_4–15 v/o TiC (inner core material) is attributed to the superposition of compressive residual stress, σ_c, in the outer layer:[12,13,19,20]

$$\sigma = AP^{-1/3} + \sigma_c \tag{4}$$

Equation (4) suggests that a plot of σ vs $P^{-1/3}$ should yield a linear relationship, and that the compressive residual stress σ_c is given by extrapolating P to zero. Figure 10 shows plots of four-point bending strength of indented samples vs $P^{-1/3}$ for both layered and monolithic samples. By extrapolating the value P to zero, it is found that σ_c for both the monolithic samples becomes close to zero, corresponding to that of stress free samples. σ_c values of 325 and 155 MPa are obtained for the layered samples with 250 and 1000 μm thickness of outer layer, respectively. The presence of compressive surface stress for a layered composite would increase the potential for inhibiting the crack growth,[12,13,21] providing another route for enhancing the flaw resistance. For example,[13] Al_2O_3–ZrO_2 layered bars with a compressive

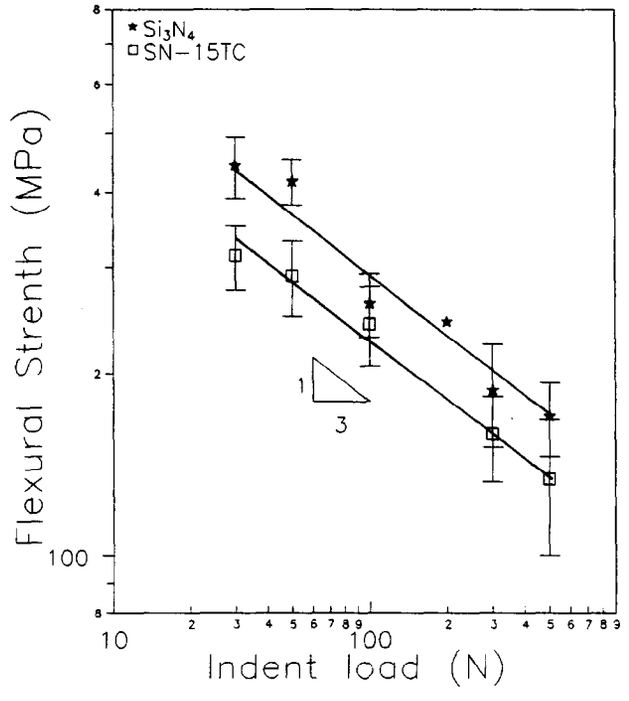

Fig. 9. Logarithmic plots of four-point bending strength of indented bars vs indent load for monolithic Si_3N_4 and Si_3N_4–15 v/o TiC ceramics.

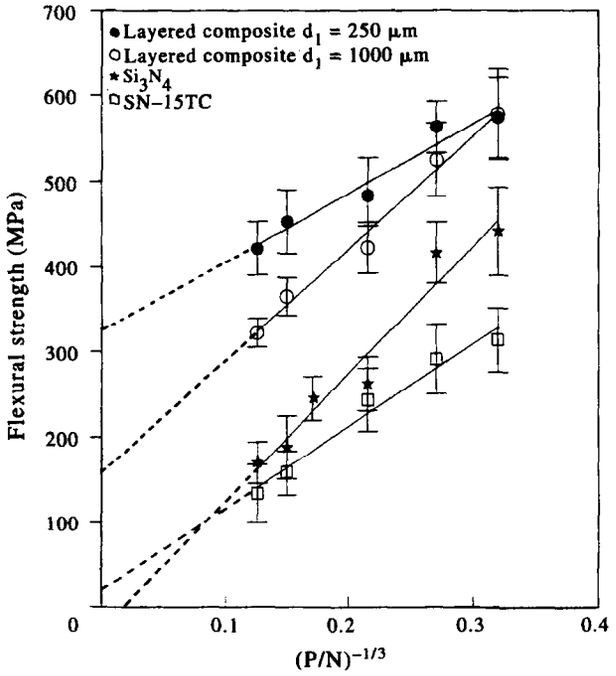

Fig. 10. Four-point bending strength vs $P^{-1/3}$ plots for the layered composites and monolithic samples.

surface stress of 550 MPa decrease in strength by only 15% after indentation with a load of 1000 N. In this work, a layered sample in the Si_3N_4–TiC system with an outer layer thickness of 250 μm obtains a higher compressive surface stress (325 MPa) and loses 30% of its initial strength after indentation with a load of 500 N, while one with 1000 μm thickness with a lower residual stress (155 MPa) loses 51% of its initial strength (Table 1).

4 CONCLUSION

Based on the present work, it is concluded that:

1. Novel layered composites in the Si_3N_4–TiC system with monolithic Si_3N_4 as the outer layers and Si_3N_4/TiC as the inner core were fabricated by slip casting and pressureless sintering.
2. The apparent viscosity of slips for the Si_3N_4–TiC system increases either with the increasing of TiC volume content or the decreasing of TiC particle size.
3. The pH values of Si_3N_4–TiC slips decrease with increasing the TiC volume content.
4. Layered composite of Si_3N_4–15 v/o TiC with a thickness of 250 μm Si_3N_4 as outer layers exhibits an excellent damage resistance, decreasing in strength by only about 30% after indentation with a load of 500 N caused by the presence of compressive surface stress.

REFERENCES

1. MAH, T., MENDIRTTA, M. G. & LIPSITT, H. A., *Am. Ceram. Soc. Bull*, **60** (1981) 1229.
2. ZILBERSTEIN, G. & BULJAN, S. T., In *Advances in Materials Characterization II, Materials Science Research*, Vol. 19, ed. R. S. Snyder, R. A. Condrate & P. F. Johnson. Plenum, New York, 1985, p. 389.
3. BULJAN, S. T. & ZILBERSTEIN, G., In *Tailoring of Multiphase and Composite Ceramics, Materials Science Research*, Vol. 20, ed. R. E. Tressler *et al.* Plenum, New York, 1986, p. 305.
4. PENI, F., CRAMPON, J., DUCLOS, R. & CALES, B., *J. Eur. Ceram. Soc.*, **8** (1991) 311.
5. HUANG, J. L., CHIU, H. L. & LEE, M. T., *J. Am. Ceram. Soc.*, **77** (1994) 705.
6. GOGOTSI, Y. G., *J. Mater. Sci.*, **29** (1994) 2541.
7. LANGE, F. F., *J. Am. Ceram. Soc.*, **63** (1980) 38.
8. GREEN, D. J., *J. Am. Ceram. Soc.*, **66** (1983) C–178.
9. VIRKAR, A. V., HUANG, J. L. & CULTER, R. A., *J. Am. Ceram. Soc.*, **70** (1987) 164.
10. CULTER, R. A., BRIGHT, J. D., VIRKAR, A. V. & SHETTY, D. K., *J. Am. Ceram. Soc.*, **70** (1987) 714.
11. VIRKAR, A. V., JUE, J. F., HANSEN, J. J. & CULTER, R. A., *J. Am. Ceram. Soc.*, **71** (1988) C–148.
12. HANSEN, J. J., CULTER, R. A., SHETTY, D. K. & VIRKAR, A. V., *J. Am. Ceram. Soc.*, **71** (1988) C–501.
13. SATHYAMOORTHY, R. & VIRKAR, A. V., *J. Am. Ceram. Soc.*, **75** (1992) 1136.
14. AMATEAU, M. F., STUTZMAN, B., CONWAY, J. C. & HALLORAN, J., *Ceram. Int.*, **21** (1995) 317.
15. FUERSTENAU, D. W., HERRERA-URBINA, R. & HANSON, J.S., In *Ceramic Powder Science II, B, Ceramic Transactions*, Vol. 1, ed. G. L. Messing, E. R. Fuller & J. H. Hausner. American Ceramic Society, Inc., OH, 1987, p. 1.
16. GREIL, P., *Mater. Sci. Eng.*, **A109** (1989) 27.
17. KRAUSE, R. F., jr, *J. Am. Ceram. Soc.*, **71** (1988) 338.
18. LI, C. W. & YAMANIS, J., *Ceram. Eng. Sci. Proc.*, **10** (1989) 632.
19. CHANTIKUL, P., ANTIS, G. R., LAWN, B. R. & MARSHALL, D. B., *J. Am. Ceram. Soc.*, **64** (1981) 579.
20. MARSHALL, D. B., LAWN, B. R. & CHANTIKUL, P., *J. Mater. Sci.*, **14** (1979) 2225.
21. GREIL, P., BOSSEMEYER, H. G. & KLUNER, A., *J. Eur. Ceram. Soc.*, **13** (1994) 159.